Title: WP7: WFI mass model plus background reduction.

Prepared by	:	E. Perinati, C. Macculi	Date :	27/02/2017
Inputs by	:		Date :	
Checked by	:	C. Macculi	Date :	27/02/2017
Agreed by	:		Date :	
Authorised by	:		Date :	

Distribution:

AHEAD WP7 leaders
AHEAD management team

DOCUMENT CHANGE RECORD

Issue	Date	Changed Section	Description of Change

Abbreviations and acronyms

Item	Meaning

Applicable Documents

[AD#]	Doc. Reference	Issue	Title
[AD1]	AHEAD project (grant agreement n. 654215)		AHEAD (Integrated Activities in the High Energy Astrophysics Domain)

Reference Documents

[RD#]	Doc. Reference	Issue	Title
[RD1]	DOI:10.1117/1.JATIS.1.1.014006		Wide Field Imager instrument for ATHENA
[RD2]	http://geant4.web.cern.ch/geant4/		Geant4 website

T a b l e O f C o n t e n t s

1 EXECUTIVE SUMMARY

In this technical note we will report on the activities related to the implementation of the Wide Field Imager (WFI) [RD1] mass model in Geant4 [RD2] to simulate the background level to be expected and identify possible technological solutions, not yet included in the ATHENA baseline, to improve the instrumental performance.

2 WFI MASS MODEL AND BKG REDUCTION

In this Section we illustrate the basic WFI mass model and summarize the result of simulations turned to assess the background level and investigate solutions to reduce it.

2.1 WFI mass model

The Wide Field Imager (WFI) developed for ATHENA is a DEPFET based detector that will provide sensitive wide field imaging in the range 0.1-15 keV, with moderate spectral resolution (<150 eV @6 keV), high time resolution (~8 μsec window mode, ~1.3 msec full frame) and high count-rate capacity (~1 Crab). It consists of a large chip 512x512 pixel with 40'x40' FOV mounted in the focus of the telescope plus a smaller fast 64x64 pixel chip defocused by 35 mm for the observation of bright sources. The other key structure is a shield where the WFI will be enclosed in order to protect it from the most damaging environmental protons, that would cause atomic displacement in the Si crystal via non ionizing energy loss.
Figure 1 shows the drawing of the basic camera head geometry, consisting of an Al shield 4 cm thick able to stop protons up to ~110 MeV.

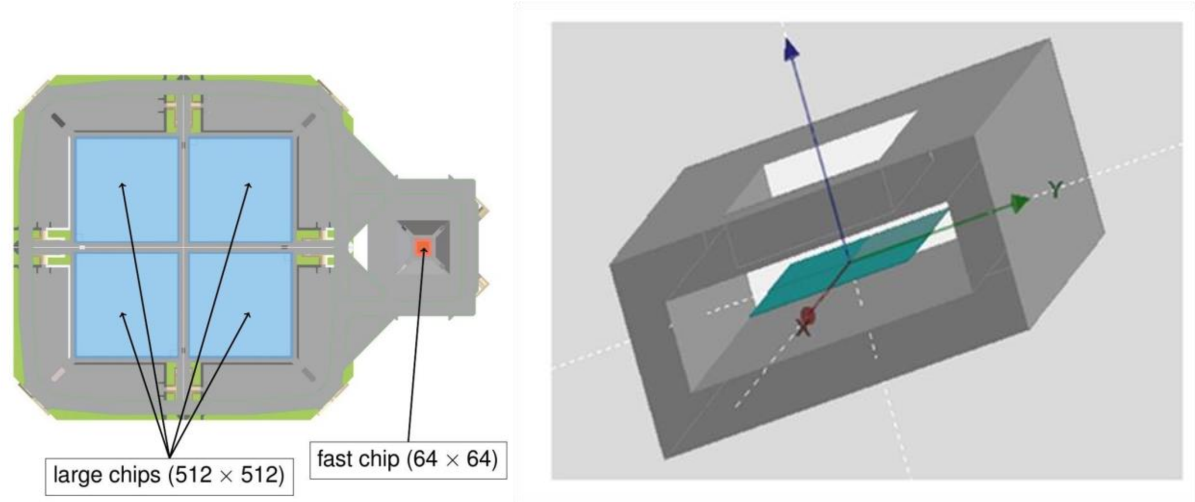

Figure 1: : the WFI basic camera head geometry (image credits:MPE).

The configuration shown in Figure 1 has been imported in Geant4.10.1.p02 and initially used to make a first-order estimation (no sub-structures, e.g. the filter-wheel, are included at this stage) of the background level and investigate how to reduce it within the requirement of $5 \cdot 10^{-3}$ cts/cm^2/sec/keV.

2.2 Solutions to reduce the WFI particle background

The following Figure 2 shows the result of simulations using as an input the average fluxes of charged particles (protons, alphas and electrons) expected at L2. The background continuum is mostly due to secondary electrons and gammas generated by the interaction of the environmental radiation with the shield, while primary particles contribute to less than 2% as they can be rejected with very high efficiency (>99.5%) thanks to the relatively large thickness of the detector. Background electrons include the very soft ones emitted with energy in the WFI band (i.e. < 15 keV) and the more energetic ones that may undergo backscattering at the detector surface, depositing only a small fraction of their energy that in some cases would fall in the WFI band. The continuum level is almost within the requirement at energies >7 keV, while at energies < 7 keV is on average ~50% higher.

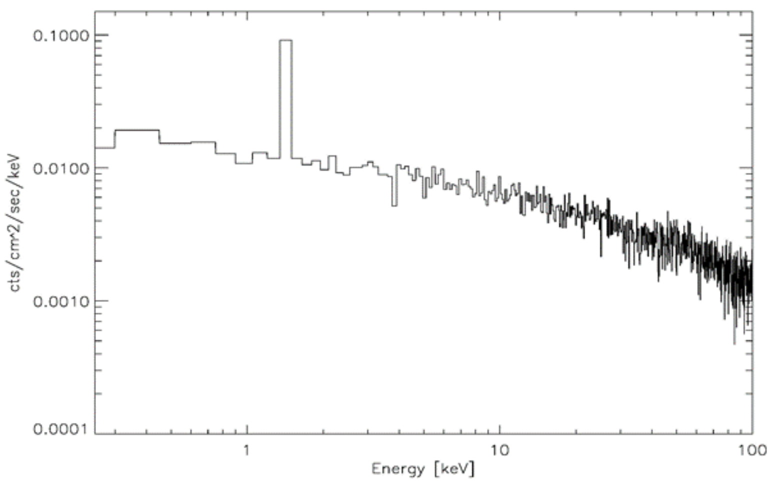

Figure 2: : background resulting from the interaction of charged particles expected at L2 with the mass model of Figure 1.

2.2.1 **The passivation**

The illuminated side of the detector will be coated with 90 nm Al as an optical/UV filter. This coating does not have much effect on the background, being able to stop only electrons up to ~1 keV. To obtain a more significant background reduction we investigated the application of a thicker passivation layer on the non-illuminated side of the detector (Figure 3).

Figure 3: : a passivation layer (orange) can be deposited on the non-illuminated side of the detector.

The layer works primarily by cutting the softer electrons emitted from the lower part of the shield that contributes a larger amount of background. To prevent electrons up to 15 keV from reaching the sensitive volume a few micron thick layer should be used, the actual thickness depends on the material. An effective and technically feasible passivation may consist of 3 μm benzocyclobutene. This helps to reduce to some extent the backscattering contribution as well, because electrons that are reflected at the surface after penetrating less than 3 μm deposit energy in the passivation. The blue line in Figure 4 shows the effect on the background. The layer does not add background by itself as it will be deposited on-chip, so that no gap is left in between, and all secondaries possibly generated in it can be rejected with the same efficiency as the primaries that generate them (assuming to fully discard frames containing primary events). The continuum effectively reduces by ~20% on average over the entire band, and by more than 30% at energies <7 keV, where the percentage of electrons in the background is higher. As a result, the reduced background falls within the requirement at energies > 7 keV and it is still just slightly higher at energies < 7 keV. However, an internal layer or graded shield not included in this simulation will be used to suppress the Al fluorescence line and possibly further reduce the continuum level as well.

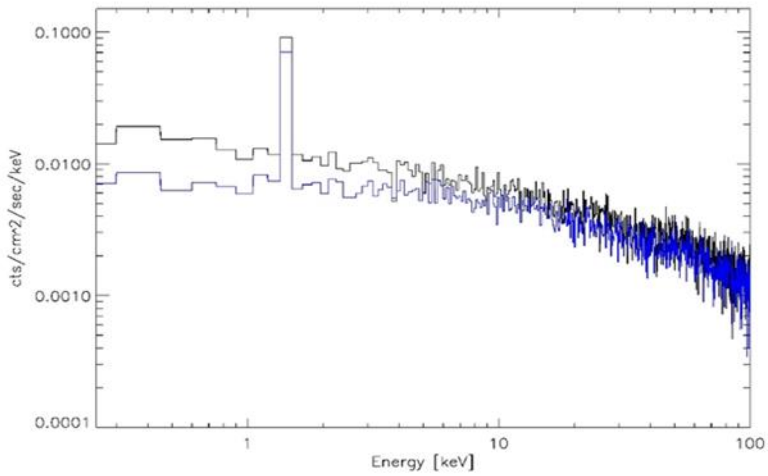

Figure 4: background resulting from the interaction of charged particles expected at L2 with the mass model of Figure 1: the cases without passivation (black line) and with passivation (blue line) are compared.

However, Geant4 simulations also showed that the drawback of the baseline configuration based on 4 cm Al is a relatively high transmissivity (~ 20 %) for diffuse high energy (~ 100 keV) photons, which can penetrate through the shield and interact with the detector via Compton scattering, making the overall background about twice as large as the requirement (Figure 5). This suggests that more work is needed to further improve the design in order to suppress this component. The background values in the different cases are summarized in Table 1. The search for solutions able to mitigate the effect of diffuse X-ray photons is ongoing and we are confident that improvements to the configuration will be considered to get rid of this component, e.g. by including a high-Z layer in the internal graded shield (Figure 6).

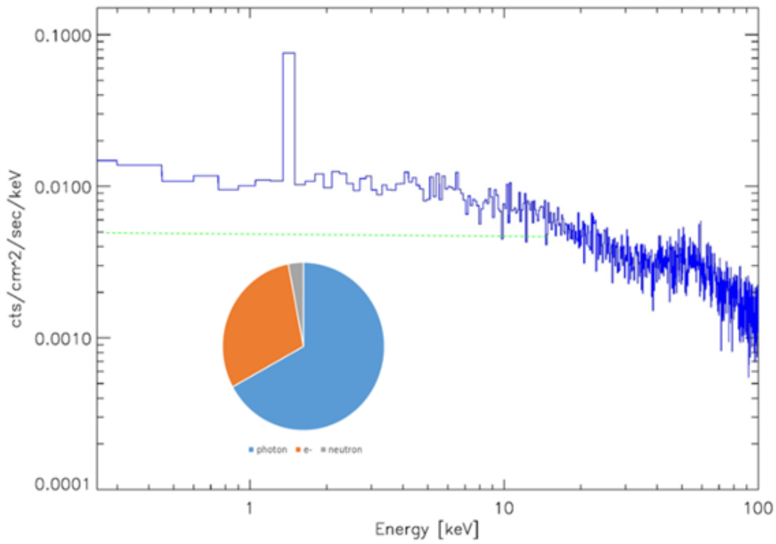

Figure 5: . Overall background induced by cosmic charged particles and diffuse X-rays (the green line indicates the requirement), the passivation on the WFI non-illuminated side is taken into account. The pie-chart shows the relative weight of the different secondary particles in the simulated WFI background. Primary particles are not taken into account as their contribution to the background is confined to border pixels

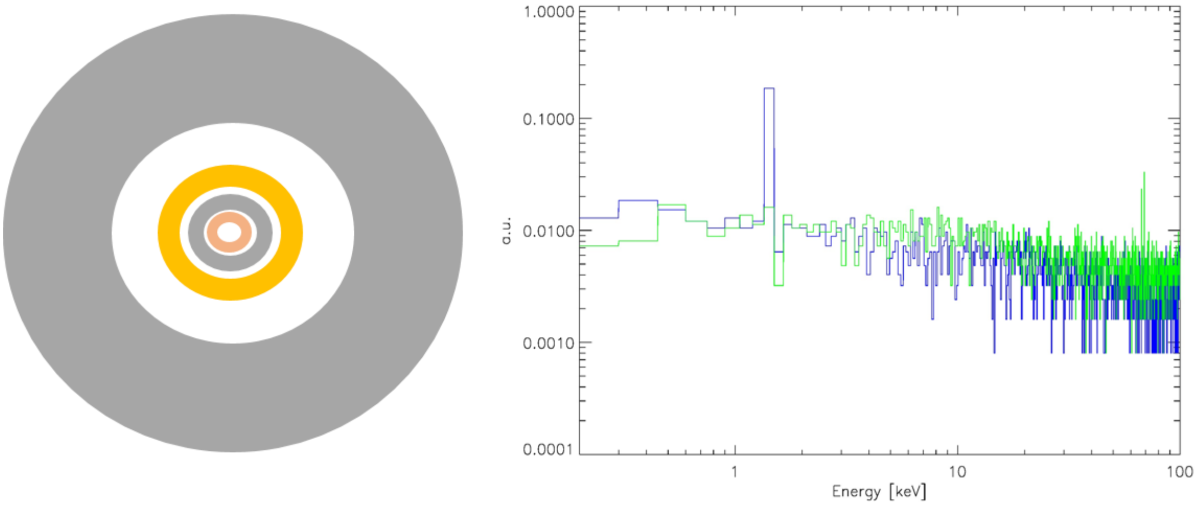

Figure 6: A possible multilayered shielding consisting of 4 cm Al (grey) + 2 mm Au (yellow) + 1 mm Al (grey) +1 mm Be (pink). In this configuration the background induced from diffuse X-ray photons is suppressed (thanks to Au), while the background induced by cosmic protons (green curve) is about the same as in the case of a 4 cm Al shell only (blue curve). However, in this configuration a flux of spallation neutrons ~3 times larger is found. The units in the plot are arbitrary as the both the background curves refer to the same closed spherical shell test geometry

charged particles (without passivation)	charged particles (with passivation)	Charged particles+diffuse X-rays (with passivation)
~0.008 cts/cm^2/sec/keV	~0.006 cts/cm^2/sec/keV	~0.01 cts/cm^2/sec/keV

Table 1. Summary of background values (average over the WFI band 0.1-15 keV).

2.2.1 **The soft electron diverter**

In a configuration more effective against diffuse X-rays, a major contribution to the background would come from secondary soft electrons emitted from the surfaces seen by WFI when primary protons pass through. These electrons are absorbed in the WFI and cannot be discriminated by pattern analysis as in most cases their mean free path is smaller than the pixel size. In the context of AHEAD we investigated a technical solution to suppress secondary soft electrons by means of a locally applied magnetic field allowing for deflection of their trajectories, so that they can be prevented from reaching the detector. The concept is described in Figure 7. Assuming that the shield is shaped as a symmetric box with four internal walls, a permanent magnet is inserted a few millimeters behind each wall seen by the WFI, producing a magnetization of the wall surface. Secondary soft electrons excited by primary protons on the wall surface are forced to move along the magnetic lines, while the secondary emission from the magnets is reabsorbed within the shield.

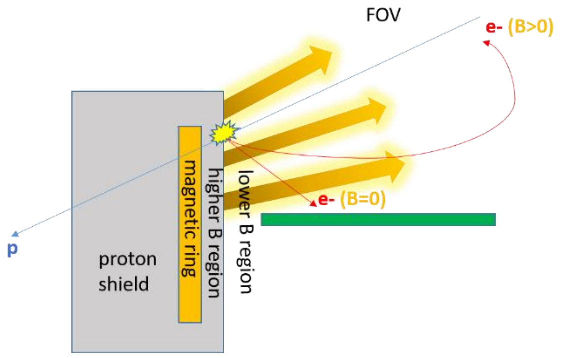

Figure 7: A permanent magnet inserted behind each shielding wall seen by the WFI produces a magnetization of the wall surface. In a four-pole field soft electrons ejected by the wall surface are forced to move along trajectories that prevent them from reaching the detector surface.

We studied the case of a single metal ring (e.g. AlNiCo) magnetized along its axis producing a four-pole field: to extend to the case of four rings it is straightforward. The four-pole field can be approximated by the field of four magnetic monopoles:

$$H_x=W*[(x-d)*(R_1^{-3}-R_3^{-3})-(x+d)*(R_2^{-3}-R_4^{-3})]$$

$$H_y= W*y*[(R_1^{-3}+R_2^{-3})-(R_3^{-3}+R_4^{-3})]$$

$$H_z= W*[(z-d)*(R_1^{-3}+R_2^{-3})-(z+d)*(R_3^{-3}+R_4^{-3})]$$

with:

$$R_1^2=y^2+(x-d)^2+(z-d)^2$$

$$R_2^2=y^2+(x+d)^2+(z-d)^2$$

$$R_3^2=y^2+(x-d)^2+(z+d)^2$$

$$R_4^2=y^2+(x+d)^2+(z+d)^2$$

$$W=0.707*H_c*d^2$$

In the expressions above H_c is the central field strength and d the distance between the poles. As a case study, we assumed a wall 7 x 16 cm (in the plane x,z) centered in x=3.5 cm, y=0.5 cm, z=0 cm and a detector 15 x 15 cm (in the plane y,z) centered in x=5 cm, y=9.5 cm, z=0. The distance between poles was set equal to 5 cm. We wrote a code in IDL to solve numerically the equations of motion of electrons in the above field. For each electron, the initial conditions (an energy in the range 0.2-15 keV, a point x_0,y_0,z_0 on the wall and a direction of motion) have been randomly generated. In all cases the coordinate x_0 has been chosen in the range 5-7 cm, as the non-illuminated side of the detector (i.e. x < 5 cm) is already shielded against soft electrons by the passivation. The efficiency of the magnetic field is defined as:

$$\varepsilon = (n_0 - n_H)/n_0$$

where n_0 and n_H are the number of electrons hitting the WFI in the cases $H_c=0$ and $H_c > 0$, respectively. Assuming that a distance of a few centimeters is left between the wall and the edge of the detector, high repelling efficiencies (> 90%) can be achieved with relatively weak fields (H_c ~100 G), thanks to the leverage effect. As an example, Figure 8 shows the simulated trajectories of some electrons having different initial conditions, for a configuration with H_c = 75 G and and 1.5 cm distance between the wall and the edge of the detector.

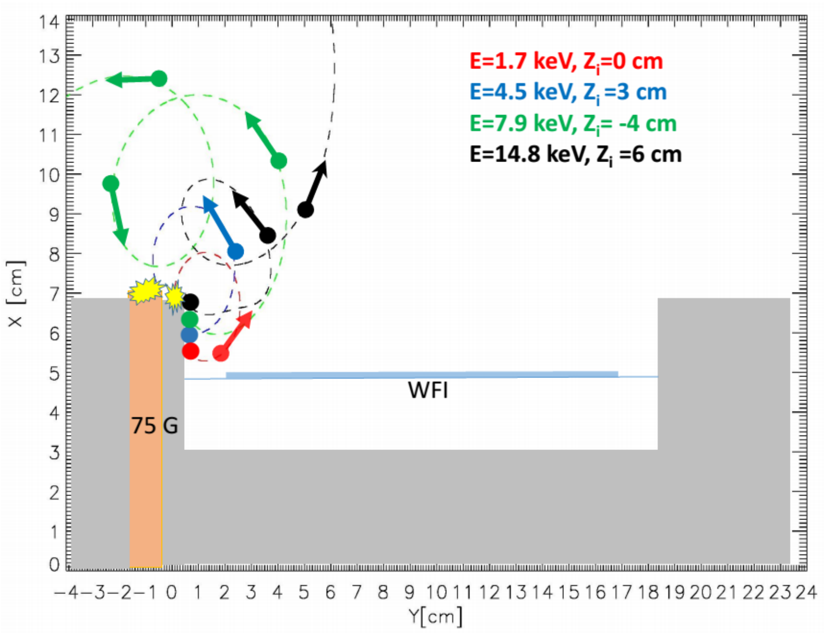

Figure 8: Simulated trajectories of some electrons with different initial conditions within the four-pole magnetic field. The central strength is 75 G.

Figure 9 shows the distribution of the residual magnetic field on the WFI for a configuration with four identical magnetic rings (one behind each wall) having the same strength at the center (H_c=75 G). The study of how such a residual field may affect the WFI functionality and the ASIC performance is beyond the scope of this work, but it should be carefully assessed in the next steps of investigation should magnetic rings be considered for implementation in the WFI camera.

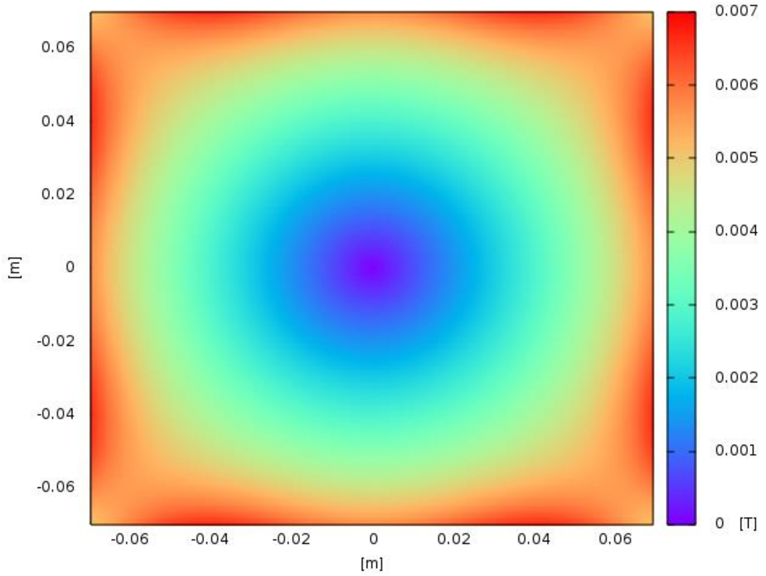

Figure 9: Distribution of the residual field on the WFI for a configuration with four identical magnetic rings (one behind each wall of the shield) having all the same central strength Hc=75 G. The residual field intensity decreases moving from the edges to the center of the detector.

4 CONCLUSION

We performed an assessment study on the background expected on the WFI. Some results obtained in this first phase of AHEAD can be considered already consolidated, e.g. the application of a passivation on the non-illuminated side of the detector is assumed in the baseline configuration. Since for technical reasons benzocyclobutene is considered the unique material suited for a passivation on the WFI, we restricted the analysis to this material. To further reduce the flux of soft secondary electrons onto the illuminated side we investigated the local application of a repelling magnetic field which may be provided by magnetic rings inserted inside the shield. Although this solution is in principle technically feasible and the study showed that it would allow to efficiently repell soft electrons, the weight that woud be added to the camera and an unavoidable residual field left on the detector are drawbacks, and further assessment would be required should such a solution be considered for implementation. The structure and composition of the internal graded shield is still under discussion, as we are currently in the phase of revising the trade off between background level and displacement damage by non ionizing energy loss, in order to improve the configuration to get rid of the diffuse X-ray contribution to the background, that the latest simulations have shown to be quite significant.